Numerical Analysis of the Non-Isothermal Flow of Polymeric Liquid between Two Coaxial Cylinders*

ALEXANDER BLOKHIN
Sobolev Institute of Mathematics
4 Academic Koptyug Avenue;
Novosibirsk State University
1 Pirogova Street,
630090 Novosibirsk
RUSSIA
blokhin@math.nsc.ru

EKATERINA KRUGLOVA
Institute of Computational Technologies
6 Academic Lavrentiev Avenue;
Novosibirsk State University
1 Pirogova Street,
630090 Novosibirsk
RUSSIA
SL2857@mail.ru

BORIS SEMISALOV
Institute of Computational Technologies
6 Academic Lavrentiev Avenue;
Novosibirsk State University
1 Pirogova Street
630090 Novosibirsk
RUSSIA
ViBiS@ngs.ru

Abstract: - Numerical simulation of the non-isothermal flow of viscoelastic polymeric liquid between two coaxial cylinders has been done on the basis of the rheological mesoscopic Pokrovskii–Vinogradov model. Boundary value problem for the nonlinear equation determining the velocity profile is posed. For solving it a pseudospectral numerical algorithm of increased accuracy based on Chebyshev approximations has been designed. The stationary numerical solutions of the posed problem are obtained for wide range of values of physical parameters and for record-low values of the radius r_0 of inner cylinder. A posteriori estimates of the truncation and round-off errors of the algorithm has been derived. Numerical analysis of these errors depending on the number of grid nodes and on the values of radius r_0 is also performed.

Key-Words: - Polymeric liquid, Pokrovskii–Vinorgadov model, Chebyshev approximation, algorithm without saturation, pseudospectral method, stabilization method, truncation error, round-off error

1 Introduction

Nowadays additive manufacturing (3D printing) can be applied to different scopes. They include health and sport industries, aviation and space applications, etc. The active development of 3D printing using polymer materials causes a need in analysis and design of new mathematical models describing with high reliability the flow of solutions and melts of polymers in the channels of printing devices. However, the macromolecular structure of polymer is very difficult. When simulating the flow of their solutions and melts for industrial applications, it is important to simultaneously take into account such properties as viscosity, anisotropy, heat transfer upon the channel walls, gravity and others. To this end we use the modified rheological Pokrovskii–Vinogradov model, which is a system of nonlinear three-dimensional equations in partial derivatives [1]. This model describes the most important properties of the flows of polymeric liquids on the basis of the mesoscopic theory of polymer dynamics, [2]–[4]. In this paper, we explore the stationary numerical solutions that are qualitatively similar to classical Poiseuille ones.

On the basis of the ideas from [5]–[7] we pose the boundary value problem for a second-order quasi-linear equation describing the distribution of the velocity of flow through the channel formed by two cylinders in the case of axial symmetry. Numerical solutions of the boundary value problem have been found by a nonlocal pseudospectral algorithm (see [8]) based on Chebyshev approximations. Numerical tests for a variety of regimes of flow have been done and the solutions for record-low values of the radius r0 of the inner cylinder have been obtained.

It is worth noting, that the asymptotic of error of Chebyshev approximations and of the nonlocal algorithm strictly corresponds to that of the best polynomial approximations [9, 10] (in Russian literature this property is known as ”the absence of saturation of the algorithm”, see [11]). This enables us to derive the reliable and accurate error estimates for approximate solutions to the considered boundary value problem and to get rich information on its main singularities. The error of numerical solution is a sum of the truncation error ε_M and the round-off error ε_R . In this work the dependence of these two errors on the number of grid nodes and on the value of r_0 is investigated up to extremely small

*This work has been done under the financial support of **Russian Science Foundation (grant agreement No. 17-71-10135)** except for the formulation of problem performed by Alexander Blokhin

values of $r_0 = 0.0002$. It should be noted, that exactly the case of extremely small r_0 (when the inner cylinder is the thin heating element) is the most prospective technological solution, allowing for controlling the flows of polymeric liquid while printing, see [7].

2 Problem Formulation

Let two cylinders with radii r_0 and 1 ($r_0 \le r \le 1$) form the channel in a 3D printing machine (see Fig. 1) and let (x, y, z) be the Cartesian coordinate system. We will consider non-isothermal flows of a polymeric liquid similar to Poiseuille ones, that are the flows under a constant pressure drop along x-axis with zero transverse components of the velocity vector and with all variables depending only on two coordinates y and z. In [6] after cumbersome transformations of the mesoscopic rheological Pokrovskii–Vinogradov model the resolving equation in cross-section of the channel was obtained. In [7] after passage to the polar coordinate system r, φ ($y = r\cos\varphi, z = r\sin\varphi$) and accounting for the axial symmetry of our problem, we have derived the following ordinary differential equation for the longitudinal component $u = u(r), 0 < r_0 \le r \le 1$, of the velocity vector

$$r\gamma u'' + \Gamma u' = -r\hat{G}K \tag{1}$$

where

$$\gamma = \frac{(1-æ^2\tilde{t}^2)(1+\tilde{t}^2)}{Q},$$
$$\Gamma = 1 + \bar{\theta}\frac{\Phi - \gamma(\bar{E}_A + \Phi)}{\ln r_0 \Phi^2},$$
$$\hat{G} = \hat{D} + \mathfrak{T}\frac{\Phi - 1}{\bar{\theta}},\ K = \frac{\tilde{K}}{J}, \tag{2}$$
$$\tilde{K} = \frac{\Lambda(1+æ^2\tilde{t}^2)}{2\tilde{t}}, \qquad \hat{D} = Re\hat{A},$$
$$æ^2 = \frac{1+\rho}{1-\rho}, \qquad \rho = 2\beta - 1,$$

β ($0 < \beta < 1$) is the phenomenological parameter of rheological model that takes into account the orientation of macromolecular coil (see [5, 6]),

$$J = \exp\left(-\bar{E}_A\frac{\Phi - 1}{\Phi}\right), \qquad \tilde{t} = \frac{1}{\tilde{g} + \sqrt{\tilde{g}^2 - 1}},$$
$$\tilde{g} = \frac{1+\sqrt{1+4\Lambda^2}}{2\Lambda}, \qquad \Lambda = \sqrt{1-\rho^2}W\bar{\tau}_0\lambda,$$
$$\bar{\tau}_0 = J/\Phi,\ \lambda^2 = (u')^2, (\lambda = |u'|), \tag{3}$$
$$Q = 1 - æ^2\tilde{t}^4 - \frac{6\rho\tilde{t}^2}{1-\rho} + \frac{4\Lambda\tilde{t}(1-\tilde{t}^2)}{1-\rho},$$

$\mathrm{G} = \frac{\mathrm{Ra}}{\mathrm{Pr}}$ (Grashof number), $\mathfrak{T} = \frac{\mathrm{Ra\ Re}}{\mathrm{Pr}}$, Ra (Rayleigh number), Pr (Prandtl number), Re (Reynolds number), $\bar{\mathrm{E}}_\mathrm{A}$ (activation energy), $\hat{A}$ (dismensionless pressure drop in the channel), W (Weissenberg number), $\bar{\theta}$ (relative temperature difference between outer and inner cylinders, if heating from the inside, then $\bar{\theta} > 0$, if heating from the outside, then $\bar{\theta} < 0$) are the constant parameters described in [5]–[7].

Remark 1 The function Φ is stationary solution of the heat conduction equation

$$\Phi_t + (\boldsymbol{u}, \nabla)\Phi = \Delta_{x,y,z}\Phi/\mathrm{Pr}, \tag{4}$$

with boundary conditions

$$\Phi = 1 + \bar{\theta}\ as\ r = r_0, \qquad \Phi = 1\ as\ r = 1.$$

Here $\boldsymbol{u} = (u, v, w)$ is the vector of velocity of the flow, $\Delta_{x,y,z}$ is Laplace operator, $\Phi = 1 + \frac{\bar{\theta}(T-T_0)}{\theta}$, $\bar{\theta} = \frac{\theta}{T_0}$, T is temperature, T_0 is the mean value of the temperature, θ is the constant temperature difference between the outer and the inner cylinders. Assuming that $\Phi = \Phi(y, z)$, $u = u(y, z)$, $v = w \equiv 0$, after passage in (4) to the polar coordinate system, one obtains $\Phi = 1 + \bar{\theta}\frac{\ln r}{\ln r_0}$.

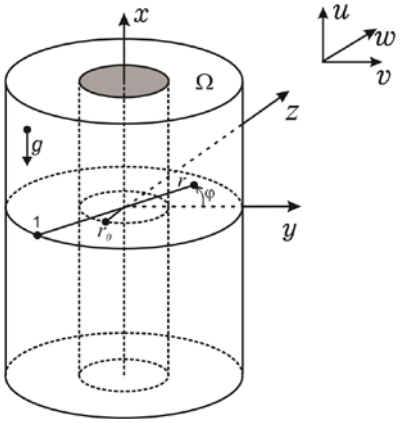

Fig. 1: Channel formed by two coaxial cylinders

It is necessary to complement the equation (1) with boundary (no-slip) conditions

$$u|_{r=r_0,1} = 0. \tag{5}$$

We pay attention to the case when r_0 is small. In this case the boundary value problem (1), (5) has

singularity in the neighborhood of the left boundary $r = r_0$ (near the wall of the inner cylinder). This singularity affects the solution significantly and presents a fundamental difficulty for the most commonly used numerical methods.

3 Design of the numerical algorithm

We rewrite (1) in the form

$$u_{rr} = (-\hat{G}K - \Gamma u_r/r)/\gamma = f(r, u_r). \quad (6)$$

For solving (6) we use the iterative time-stepping stabilization technique. To this end, we introduce a fictive time variable t that will be used for iterations and the regularizing operator (the regularization) B_t. Assuming that $u = u(r,t)$ we seek the solution of (6) as the limit of solutions of the evolution equation

$$B_t u = u_{rr} - f(r, u_r) \quad (7)$$

as $t \to \infty$.

Here B_t is the Sobolev's regularization $B_t = \left(k_1 - k_2 \frac{\partial^2}{\partial r^2}\right)\frac{\partial}{\partial t}$, where $k_1, k_2 > 0$ are constants. Introducing the grid with respect to t with the step τ and the nodes $t_n = n\tau$, $n = 1,2,\ldots$ and denoting $u^{[n]} = u^{[n]}(r) = u(r, t_n)$ we approximate the derivative u_t by the difference relation $(u^{[n]} - u^{[n-1]})/\tau$. As a result, we obtain the following formula

$$k_1 u^{[n]} - (k_2 + \tau)u^{[n]}_{rr} = \left(k_1 - k_2 \frac{\partial^2}{\partial r^2}\right)u^{[n-1]} - \tau f\left(r, u^{[n-1]}_r\right) = \tilde{f}\left(r, u^{[n-1]}\right). \quad (8)$$

The idea of method consists in finding the solution $u^{[n]}$ of (8) on the current time step using its values $u^{[n-1]}$ from the previous step. These operations are repeated until the difference between the solutions at the previous and next time steps becomes small enough. We use the stopping criteria

$$\|B_t u\| < \varepsilon_S, \quad (9)$$

where ε_S is the error (or residual) of the stabilization process, $\|\cdot\|$ is the uniform norm of function (it is assumed to be continuous). Below we use $\varepsilon_S = 10^{-14}$.

To approximate the function u and its derivatives with respect to r in regularized equations the modified interpolation polynomial with Chebyshev nodes written in the Lagrange form is used

$$u(r) \approx p(u,r) = \sum_{j=1}^{N} \frac{s(\tilde{r}, r_j)T_N(\tilde{r})}{(\tilde{r} - r_j)T_N'(r_j)} u(\tilde{r}_j),$$
$$s(\tilde{r}, r_j) = \frac{1-\tilde{r}^2}{1-\tilde{r}_j^2},\ r_j = \cos\frac{2j-1}{2N}\pi, \quad (10)$$

where $T_N(\tilde{r}) = \cos(N\arccos\tilde{r})$, $\tilde{r} = \frac{2}{1-r_0}\left(r - \frac{1+r_0}{2}\right) \in [-1,1]$, $\tilde{r}_j = r_j\frac{1-r_0}{2} + \frac{1+r_0}{2}$.

The factor $s(\tilde{r}, r_j)$ automatically provides accounting for homogenous boundary conditions (5) for function u, therefore we called the polynomial (10) as "modified".

For solving the equation (8) we use the expansion (10) and the collocation method. The expansion (10) was differentiated with respect to r. Further we shall use the notations $U = U^{[n]} = \left(u(\tilde{r}_1), \ldots, u(\tilde{r}_N)\right)^T$, $U_r = \left(u'(\tilde{r}_1), \ldots, u'(\tilde{r}_N)\right)^T$, $U_{rr} = \left(u''(\tilde{r}_1), \ldots, u''(\tilde{r}_N)\right)^T$. Here the upper index "$[n]$" of the components of vectors is omitted.

$$p'(u,r) = \frac{2}{1-r_0}\sum_{j=1}^{N}(-1)^{j-1}u_j \cdot \cdot \left\{\frac{2\tilde{r}r_j - \tilde{r}^2 - 1}{N(\tilde{r} - r_j)^2 q_j}T_N(\tilde{r}) + \frac{q}{q_j(\tilde{r} - r_j)}\sqrt{1 - T_N^2(\tilde{r})}\right\}, \quad (11)$$

$$p''(u,r) = \frac{4}{(1-r_0)^2}\sum_{j=1}^{N}(-1)^{j-1}u_j \cdot \cdot \left\{\frac{2q_j^2 - N^2(\tilde{r} - r_j)^2}{N(\tilde{r} - r_j)^3 q_j}T_N(\tilde{r}) - \frac{(\tilde{r}^2 - 3\tilde{r}r_j + 2)}{q q_j(\tilde{r} - r_j)^2}\sqrt{1 - T_N^2(\tilde{r})}\right\}, \quad (12)$$

where $q = \sqrt{1 - r^2}$, $q_j = \sqrt{1 - r_j^2}$.

The limit expressions of the first-order and of the second-order derivatives (11), (12) as $r \to \tilde{r}_i$ were obtained using l'Hospital's rule.

$$p'(u, r_i) = C_{r0}\left(\sum_{\substack{j=1 \\ j\neq i}}^{N}(-1)^{i+j}\mathfrak{a}_{ij}u_j - \mathfrak{n}_i u_i\right),$$
$$p''(u, r_i) = C_{r0}^2\left(\sum_{\substack{j=1 \\ j\neq i}}^{N}(-1)^{i+j-1}a_{ij}u_j - \nu_i u_i\right),$$

where

$$C_{r0} = \frac{2}{1-r_0},\ \mathfrak{a}_{ij} = \frac{(-1)^{i+j} q_i}{q_j (r_i - r_j)},$$
$$a_{ij} = (-1)^{i+j} \frac{2q_i^2 + 3r_i(r_i - r_j)}{q_j q_i (r_i - r_j)^2}, \quad (15)$$
$$i, j = 1, \dots, N, i \neq j,$$

$$\mathfrak{n}_i = -\frac{3r_i}{2q_i^2}, \quad (16)$$
$$\nu_i = -((N^2+5)q_i^2 + 3r_i^2)/(3q_i^4),\ i = 1, \dots, N.$$

Now we can form the $N \times N$ matrices

$$\mathfrak{A} = C_{r0} \begin{pmatrix} \mathfrak{n}_1 & \mathfrak{a}_{12} & \cdots & \mathfrak{a}_{1N} \\ \mathfrak{a}_{21} & \mathfrak{n}_2 & \cdots & \mathfrak{a}_{2N} \\ \vdots & \vdots & \cdots & \vdots \\ \mathfrak{a}_{N1} & \mathfrak{a}_{N2} & \cdots & \mathfrak{n}_N \end{pmatrix}, \quad (17)$$

$$A = C_{r0}^2 \begin{pmatrix} \nu_1 & a_{12} & \cdots & a_{1N} \\ a_{21} & \nu_2 & \cdots & a_{2N} \\ \vdots & \vdots & \cdots & \vdots \\ a_{N1} & a_{N2} & \cdots & \nu_N \end{pmatrix} \quad (18)$$

approximating the first-order and the second-order derivatives:

$$U_r \approx \mathfrak{A}U, U_{rr} \approx AU. \quad (19)$$

We construct the algorithm, using the spectral decomposition of the matrix A approximating the second-order derivatives:

$$A = R_A D_A R_A^{-1}, \quad (20)$$

where R_A is the matrix of eigenvectors of A; D_A is the diagonal matrix containing the eigenvalues d_A^j of $A, j = 1, \dots, N$. The decomposition (20) should be done once before running the iterative process. This helps us to reduce the computational costs of the algorithm.

Solving (8) by using (10) and collocation method we reduce our problem to the problem of linear algebra with the matrix $k_1 E - (k_2 + \tau)A$ (E is the identity matrix). Multiplying this system by the matrix R_A^{-1} from the left, we have

$$k_1 V^{[n]} - (k_2 + \tau) D_A V^{[n]} = G^{[n]}, \quad (21)$$

where $V^{[n]} = R_A^{-1} U^{[n]}, G^{[n]} = R_A^{-1} \tilde{F}(U^{[n-1]})$ are vectors of the size N, $\tilde{F} = \tilde{F}(U^{[n-1]})$ is the vector of values of $\tilde{f}(r, u^{[n-1]})$ in the collocation nodes $\tilde{r}_j$, $j = 1, \dots, N$. As a result, we come to the formula expressing the components of the vector $V^{[n]}$ through the values of components g_j of the vector $G^{[n]}$:

$$v_j = \frac{g_j}{k_1 - (k_2 + \tau) d_A^j}, j = 1, \dots, N. \quad (22)$$

After finding the components of the vector $V^{[n]}$ on the nth time step, we can get the solution: $U^{[n]} = R_A V^{[n]}$. The formulas (22) imply that the conditions necessary for convergence of the proposed method are satisfied, i.e.

$$\tau \neq \frac{k_1}{d_A^j} - k_2, \forall j. \quad (23)$$

Note, that the number of operations required for computing the solution on each time step is determined by the products of matrices and vectors, namely $G^{[n]} = R_A^{-1} \tilde{F}(U^{[n-1]})$ and $U^{[n]} = R_A V^{[n]}$. It is equal to $2N^2$ by the order of the magnitude of N.

A significant advantage of the proposed algorithm is the use of (10). It guarantees, that the numerical solution will asymptotically satisfy the estimates of error of the best polynomial approximations for any order of smoothness (or regularity) of the desired solution. More precisely, in the case of finite order of smoothness ($u \in C^r[r_0, 1]$), we get the *algebraic rate of convergence* of the order $\rho \in [r, r+1]$, [9, 10]; in the case of infinite smoothness *the geometric rate of convergence* can be achieved for functions with singularities in the complex plain and *the super-geometric rate* is observed for entire functions, see [12,13]. In numerical tests we checked, that our algorithm does not reduce the rate of convergence of its approximation while solving differential equations, i.e. its rate is close to that for the best polynomial approximations. Therefore, the algorithm *does not have saturation* [11], that enables us to set the strict correspondence between its rate of convergence and the order of smoothness (or regularity) of the sought-for solution and also gives an opportunity to use the error estimates of the best polynomial approximations for calculating the truncation error. Thereby, the described algorithm enables us to obtain the approximate solution to the problem (1), (5) with the error control for record-low values of r_0 (which is the most important for industrial applications).

4 Estimation of the round-off error

The implementation of any method on computer with floating point arithmetic implies the rounding of real numbers. The reason is that the length of mantissa of real number in the computer's memory

is always restricted by finite number of digits l (usually for float format l=8, for double format l =16, for quadruple format l =32, etc). All the digits that do not fit within these restrictions are dropped and, while writing the number a into computer's memory, this causes the occurrence of the error δ_a, i.e. $a \to a + \delta_a$. The value δ_a is usually unknown, but there is the estimate $|\delta_a| \le \delta|a|$, where δ is the relative round-off error, $\delta = 10^{-l+1}$. During calculations the round-off errors accumulate. It may lead to the catastrophic loss of accuracy. Thus, one needs the reliable and accurate estimate describing the behavior of round-off error ε_R of the obtained solution. Such estimates are usually derived for problems of linear algebra using the methods of interval analysis [14, 15], or by means of construction of a priory estimates [16, 17].

In order to estimate ε_R in our problem, let us recall the way of finding a solution to regularized equation (8) after its discretization:

$$U^{[n]} = (k_1 E - (k_2 + \tau)A)^{-1}\tilde{F}\left(U^{[n-1]}\right) \Rightarrow U^{[n]} = S\left(U^{[n-1]}\right), \quad (24)$$

where $S: \mathbb{R}^N \to \mathbb{R}^N$ is the nonlinear operator.

We assume that the system of nonlinear equations written in collocation nodes has the solution. It means, that the sequence of solutions $U^{[n]} \in \mathbb{R}^N$ under the action of operator S should converge to the vector $U^{[n]} \in \mathbb{R}^N$ of values of polynomial $p(u,r)$ (see (10)) in collocation nodes, that satisfy exactly the initial nonlinear equation (1) in these nodes. The necessary and sufficient condition for such convergence is the requirement for S to be *the contraction mapping*.

According to the Banach fixed-point theorem, if S is the contraction mapping, then it has the unique fixed point and the stabilization iterations converge uniformly with geometric decay of the error. We use this fact to construct the round-off error estimate. Let us consider the Fig. 2.

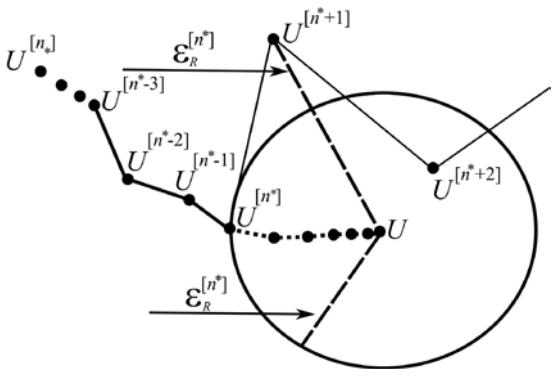

Fig. 2: Convergence of the stabilization method to the solution U

On the time step n^*, when $U^{[n^*]}$ approaches close enough to the vector U (in the Figure this domain is denoted by oval), the uniform convergence fails. The subsequent solutions may leave this domain (the example is denoted by thin solid line) moving away from the solution U further, than they were on the previous time steps. This happens by virtue of the round-off error ε_R. In case of absence of ε_R the sequence $U^{[n]}$ would continue to converge to solution U with the geometric decay of the norm $\left\|U^{[n]} - U^{[n-1]}\right\|$ as the dashed line shows.

The idea is to estimate the length of the path from $U^{[n^*]}$ to U. This length is the sum of lengthes of the segments denoted by dashed line. As soon as the given stabilization residual is reached, i.e. the inequality (9) is satisfied, we denote the number of this step by $n = n_*$ and search the step $n^* > n_*$ such that $[n_*, n^*]$ is the largest segment of uniform convergence observed in numerical test. By the following formulas

$$z_n = \frac{\left\|U^{[n+1]} - U^{[n]}\right\|}{\left\|U^{[n]} - U^{[n-1]}\right\|}, \quad (25)$$
$$\chi^N_{max} = \max_{n=n_*,\dots,n^*}(z_n), U^{[n]} \in \mathbb{R}^N,$$

we calculate z_n while n increases starting from n_*. If z_n<1, then the convergence is uniform. If $z_n \ge 1$, i.e. the solution lays on the oval in Fig. 2, then the uniform convergence fails and the current $n = n^*$ (these arguments are correct only if the parameters k_1, k_2, τ are chosen so that the convergence begins with the first step). In this moment we stop the iterations and computation of z_n and calculate χ^N_{max}. The obtained value of χ^N_{max} approximates the Lipschitz constant of $S(U)$ with high accuracy, since it is computed as a maximum over a large number of iterations $\mathbb{K} = n^* - n_*$ (in our tests $\mathbb{K}$>50 always). Let $\varepsilon_R^{[n^*]}$ be the estimate of the distance from $U^{[n^*]}$ to U. According to the Banach fixed-point theorem one has

$$\varepsilon_R^{[n^*]} \le \frac{\left\|U^{[n^*]} - U^{[n^*-1]}\right\|}{1 - \chi^N_{max}} \quad (26)$$

Below we estimate the growth of the round-off error ε_R while passing to the next $(n^* + 1)$th step. This characterizes the numerical stability of the proposed algorithm. To this end we carefully analyzed the scheme of algorithm and took into account that the multiplication of matrices by

vectors AU gives the following round-off error: $\|\delta_{AU}\| \le N_A^{\infty}(\delta\|U\| + \|\delta_U\|)$, where δ_{AU} is the matrix with elements $(\delta_{AU})_{ij}$ that are the numerical disturbances of the elements of matrix AU caused by the round-off error, δ_U is the vector with components $(\delta_U)_j$ that are the numerical disturbances of the components of vector U, $N_A^{\infty} = \|A\|_{\infty} = \max_{j=1,\dots,N} \sum_{j=1}^{N} |a_{ij}|$.

By using the estimate $|\delta_a| \le \delta|a|$ and the Taylor expansion of the disturbances of each operation from the right hand side of (6) in the vicinity of $\delta = 0$ and by taking only the linear part of this expansion, we finally derived the estimate of $\left\|\delta_{\tilde{F}}\left(\varepsilon_R^{[n^*]}\right)\right\|$. It enabled us to calculate the following a posteriori estimate:

$$\varepsilon_R^{[n^*+1]} \le \delta\, N_{R_A}^{\infty} \left\|V^{[n^*+1]}\right\| + cond_{R_A}^{\infty} \frac{\delta\left\|\tilde{F}\left(\varepsilon_R^{[n^*]}\right)\right\| + \left\|\delta_{\tilde{F}}\left(\varepsilon_R^{[n^*]}\right)\right\|}{\min_j |k_1 - (k_2+\tau)d_A^j|}. \quad (27)$$

Here $cond_{R_A}^{\infty}$ is the condition number of matrix R_A. $\tilde{F}$ is a vector containing the values of right hand side of (6).

5 Estimation of the truncation error

It is worth noting that the exact solution of (1) can't be obtained by analytical methods. Therefore, the rate of convergence of the proposed algorithm could be estimated by Runge's rule, which requires the increase of the number of collocation nodes in two times. This may lead to significant growth of computational costs. Therefore, we shall consider the modification of Runge's rule. Let us increase the number of nodes N by unity and observe the value of $\|P_{N+1}(u) - P_N(u)\|$, where u is the exact solution of the problem (1), (5) and $P_N(u) = P_N(u)(r)$ is its approximation of the form (10) that was obtained by the described algorithm with N collocation nodes. Thus, the following estimates take place

$$\begin{aligned} &\|P_N(u) - u\| \le \|P_N(u) - P_{N+1}(u)\| + \\ &+\|P_{N+1}(u) - u\|, \\ &\|P_N(u) - u\| - \|P_{N+1}(u) - u\| \le \\ &\le \|P_N(u) - P_{N+1}(u)\|, \\ &\varepsilon_M = \|P_N(u) - u\| \le \frac{1}{1-\varkappa_N}\|P_N(u) - P_{N+1}(u)\|. \end{aligned} \quad (28)$$

Here $\varkappa_N = \frac{\|P_{N+1}(u)-u\|}{\|P_N(u)-u\|}$, then $\varkappa_N\varkappa_{N-1} = \frac{\|P_{N+1}(u)-u\|}{\|P_{N-1}(u)-u\|}$. As the Chebyshev approximation is uniform, we use the following expression

$$\begin{aligned} \varkappa_N\varkappa_{N-1} &\sim \frac{R_{N+1}(r)}{R_{N-1}(r)}, \\ R_N(r) &= |P_N(r) - u(r)|, \\ P_N(r) &= P_N(u)(r), \end{aligned} \quad (29)$$

where $r \in [r_0, 1]$ is an arbitrary point that does not coincide with any of collocation nodes, the sign '$\sim$' means the asymptotical equivalence for large N. Taking into account the absence of saturation of the proposed algorithm (i.e. that the asymptotic of its error strictly corresponds to that of the best polynomial approximations) one can conclude, that for N large enough three types of asymptotical estimates for $\varkappa_N$ are possible:

1) if $u \in C^r([r_0, 1])$, then according to Jackson inequality [9, 10] the algebraic convergence takes place, i.e. one has $\varkappa_N \sim \frac{(N+1)^{-r}}{N^{-r}} = \frac{N^r}{(N+1)^r}$; ;

2) if $u \in C^{\infty}([r_0, 1])$, has singularity in the complex plane, then according to Bernstain's results [12, 18] the geometric convergence takes place, i.e. one obtains $\varkappa_N \sim \frac{q^{N+1}}{q^N} = q < 1$;

3) if u is entire and its Nth derivative is bounded by the power function $\left\|u^{(N)}\right\| \le c^N$, then the estimates of the error of interpolation from [19] yield

$$\varkappa_N \sim \frac{\tilde{q}^{N+1}}{(N+1)!} \Big/ \frac{\tilde{q}^N}{N!} = \frac{\tilde{q}}{N+1},\ \tilde{q} > 0 \text{ depends on } c.$$

Let N be odd, then 0 is the node of P_N. We substitute these values into (29) and have

$$R_N(0) = 0, \qquad |R_{N+1}(0)| = \varkappa_N\varkappa_{N-1}|R_{N-1}(0)|.$$

Solving our boundary value problem with $N-1, N, N+1$ collocation nodes and accounting for $|P_N(r) - P_{N+1}(r)| = |R_N(r) - R_{N+1}(r)|$ we introduce the quantity λ_N:

$$\lambda_N = \sqrt{\frac{|P_N(0) - P_{N+1}(0)|}{|P_{N-1}(0) - P_N(0)|}}. \quad (30)$$

Here

$$\begin{aligned} \lambda_N &= \sqrt{\frac{|R_N(0) - R_{N+1}(0)|}{|R_{N-1}(0) - R_N(0)|}} \\ &= \sqrt{\frac{|R_{N+1}(0)|}{|R_{N-1}(0)|}} \sim \sqrt{\varkappa_N\varkappa_{N-1}}. \end{aligned} \quad (31)$$

There are three types of asymptotic relations between λ_N and $\varkappa_N$ for the mentioned types of convergence:

In the first case one has $\left|\varkappa_N^2 - \varkappa_N\varkappa_{N-1}\right| = \frac{|N^{2r}-(N^2-1)^r|}{(N+1)^{2r}} \sim \frac{r}{N^2}$ as $N \to \infty$. Therefore $\lambda_N \to \varkappa_N \to 1$ and $r \sim \log_{\frac{N}{N+1}} \lambda_N$ as $N \to \infty$.

In the second case $\varkappa_N \sim \varkappa_{N-1} \sim q$, it means that $\lambda_N \to \varkappa_N \to q$ as $N \to \infty$. , where $0 < q < 1$.

In the third case $\left|\varkappa_N^2 - \varkappa_N\varkappa_{N-1}\right| \sim \frac{\tilde{q}^2}{N(N+1)^2}$. Hence, $\lambda_N \to \varkappa_N \to q$ as $N \to \infty$.

For all of the considered cases we have $\lambda_N \to \varkappa_N \to q$ as $N \to \infty$. This means that observing the value of λ_N for N large enough, one can make the conclusions on the rate of convergence and consequently on the order of smoothness (or regularity) of the desired solution based on these observations. To calculate the right hand side of (28) one needs to know the value of norm $\|P_{N+1}(u) - P_N(u)\|$. This value has been obtained in two steps. Firstly, the roots of $P_{N+1}(u) - P_N(u)$ were found. Secondly, using the fundamental theorem of algebra, their extremes were located and obtained. On both steps the bisection method was used. Numerical tests showed, that this method is the most simple and stable for our problem.

6 Numerical tests

The described algorithm together with methods of computation of the errors was implemented in Matlab. The program has been run on the computer Intel Core i5-3337U, 1.8 GHz, 6 Gb DIMM DDR3 RAM. During this investigation a variety of the stationary regimes of polymeric fluid flow has been simulated (see also [7]). Below we present the analysis of some of these solutions depending on the values of two parameters (they are the Weissenberg number W and the dimensionless temperature difference $\overline{\theta}$) that have strong influence on the flow. Here we set $\beta = 0.1, \widehat{D} = -1, E_A = 9, r_0 = 0.5$.

Figures 3, 4 present the dependence of the velocity of polymeric liquid $u(r)$ on the radial coordinate r (graph a), the dependance of the modulus of rate of flow (graph b) and the maximum value of modulus of velocity (graph c) on the parameters W and $\overline{\theta}$.

For small values of W (points 1,2) the profiles are almost identical, the flow rate decreased insignificantly. With the increase of Weissenberg number, the velocity profile becomes more convex, which is due to the activation effect and the macromolecular structure of the polymers (see Fig. 3).

From the Fig. 4 it can be seen how different forms of heating affect the flow of polymeric liquid. For $\overline{\theta} > 0$ we have the heating of the inner cylinder wall, for $\overline{\theta} < 0$ the heating of the outer cylinder wall. In the case of heating from outside, the velocity profile $u(r)$ is small. However, as soon as $\overline{u}$ is positive, the velocity and the flow rate increase rapidly. It should be noted, that as heating of the inner wall increases, the profiles become less symmetric. This provides a new way for controlling the flows of polymeric liquid during 3D printing and presents a prospective technological solution for additive manufacturing.

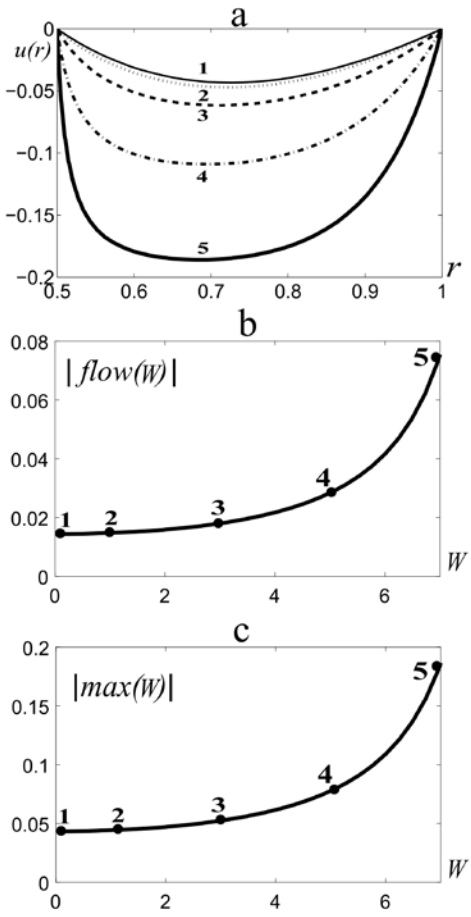

Fig. 3: Numerical analysis of the polymeric fluid flow for $\overline{\theta} = -0.01$ and different values of W: $W = 0.01$ (point 1), $W = 1$ (point 2), $W = 3$ (point 3), $W = 5$ (point 4), $W = 7$ (point 5). Here are the velocity of flow vs. the coordinate r (graph a); the rate of flow vs. W (graph b) and the maximum velocity of flow vs. W (graph c)

In this work we also got the estimates of the truncation and round-off errors for the regime of flow with $\beta = 0.1, \widehat{D} = -1, E_A = 9, W =$

$0.01, \overline{\theta} = -0.01$, while the values of r_0 were decreasing starting from $r_0 = 0.2$ up to $r_0 = 0.0002$ (see Figure 5). Firstly we compute the values of solution $u(\tilde{r}_j)$, $j = 1, \ldots, N$ using the described algorithm. Then, applying the formulas from the previous sections for these solutions we compute the estimates of truncation and round-off errors ε_M and ε_R, depending on the number of collocation nodes N.

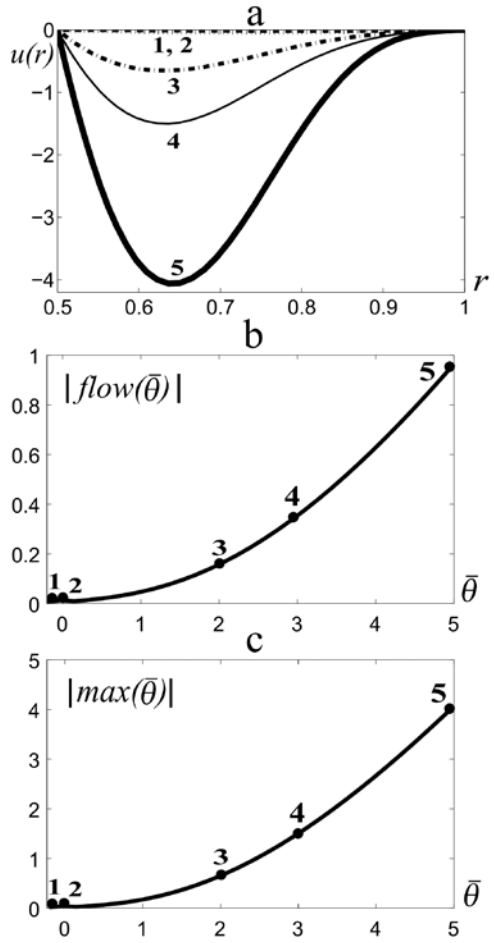

Fig. 4: Numerical analysis of the polymeric fluid flow for $W = 0.01$ and different values of $\overline{\theta}$: $\overline{\theta} = -0.2$ (point 1), $\overline{\theta} = -0.01$ (point 2), $\overline{\theta} = 2$ (point 3), $\overline{\theta} = 3$ (point 4), $\overline{\theta} = 5$ (point 5). Here are the velocity of flow vs. the coordinate r (graph a); the rate of flow vs. $\overline{\theta}$ (graph b) and the maximum velocity of flow vs. $\overline{\theta}$ (graph c).

Characteristic $\widehat{D}$ of the pressure gradient and of the liquid viscosity for these tests was negative, therefore the velocity profiles are directed downwards. In Fig. 5 the large gradients caused by the presence of the small value of r_0 in (1) near the inner cylinder wall can be observed. They are these gradients that cause the high complexity for many computational methods.

In Fig. 6 the values of λ_N ($N \in \mathbb{N}\, is\, odd$) are shown for the three tests. From the graphs it can be seen that for small values of N the oscillations of λ_N are not large, and the convergence of them to some limit values $q = \lim_{N\to\infty} \lambda_N$ takes place. For large values of N, when the truncation error decreases up to the values $10^{-14} - 10^{-10}$, the large chaotic oscillations of λ_N caused by the round-off error are observed. Let N_0 be the minimal value of N, ensuring the convergence of the stabilization method; N_1 be the value of N in which the chaotic oscillations start (it can be easily seen in the graphs). For determining the value of q for the truncation error estimation we have approximated the values of λ_N on the segment $[N_0, N_1]$ using the function

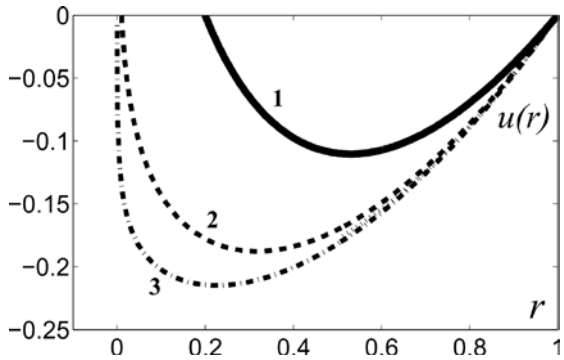

Fig. 5: Numerical solutions to the problem (1), (5) with $\beta = 0.1, \widehat{D} = -1, E_A = 9, W = 0.01$, $\overline{\theta} = -0.01$ ($\mathfrak{T} = -1$) for different values of r_0 ($r_0 = 0.2$ is the test No. 1, $r_0 = 0.01$ is test No. 2, $r_0 = 0.0002$ is test No. 3)

$$At(N) = b_1 \arctan(b_2 N + b_3) + b_4. \quad (32)$$

The coefficients $b_1 - b_4$ were derived using the methods of nonlinear non-convex optimization implemented in OPTCON program package, see [20]. Minimization of the mean square deviation (MSD) between the approximation $At(N)$ and the data λ_N was done over all odd N in the segment $[N_0, N_1]$. Taking into account that $\arctan(x) \to \pi/2\ as\ x \to \infty$, we approximate the value of q with a value $\hat{q} = b_1\pi/2 + b_4$ (these values of $\hat{q}$ are shown in Fig.6). By observing MSD we can draw conclusions on the accuracy of approximation (32). Note that in order to avoid mess in the Fig. 6, a considerable number of points presenting the values of λ_N was not put on the graph c, but all these values were taken into account, while computing the function $At(N)$. The values of N_0, N_1, $b_1 - b_4$, $\hat{q}$

and MSD obtained for the three considered tests are given in Table 1.

In Fig. 7 the estimates of the truncation and round-off errors are given in logarithmic scale. From the graphs it can be seen, that while N is increasing, the values of ε_M show the geometric decay, and the values of ε_R grow approximately as the power function of N. This is caused by power growth of the norms of matrices approximating the derivatives that that enter the expression of right part in the estimate (27).

Table 1: Parameters of the approximation $At(N)$

r_0	$[N_0, N_1]$	b_1	b_2	b_3	b_4	$\hat{q}$	MSD
0.2	[10, 30]	0.858	2.267	-17.733	-1.0	**0.34**	8.7e-04
0.01	[10, 110]	0.170	0.200	-1.986	0.550	**0.8170**	5.8e-04
0.0002	[196,N], $N > 340$	0.055	0.071	-3.496	0.886	**0.9724**	3.4e-07

7 Conclusion

In this work, the pseudospectral algorithm without saturation has been designed that enables us to simulate the stationary regimes of polymeric liquid flow between two coaxial cylinders with extremely small values of the radius of the inner cylinder r_0 and with other parameters varying in wide ranges. These results are aimed at the development of the state-of-the-art technological solutions for the additive manufacturing industry.

The absence of saturation of the proposed algorithm and the geometric rate of convergence of Chebyshev approximation confirmed by numerical tests ensure that the solution is infinitely smooth function having singularity in the complex plain. Moreover, the distance from it to the real value interval of the problem decays while the radius of inner cylinder decreases. The high numerical stability of the proposed algorithm is proved by the slow growth of the round-off error with the growth of number of collocation nodes. We believe that both the obtained numerical solutions and a posteriori estimates of their errors will be useful for practice.

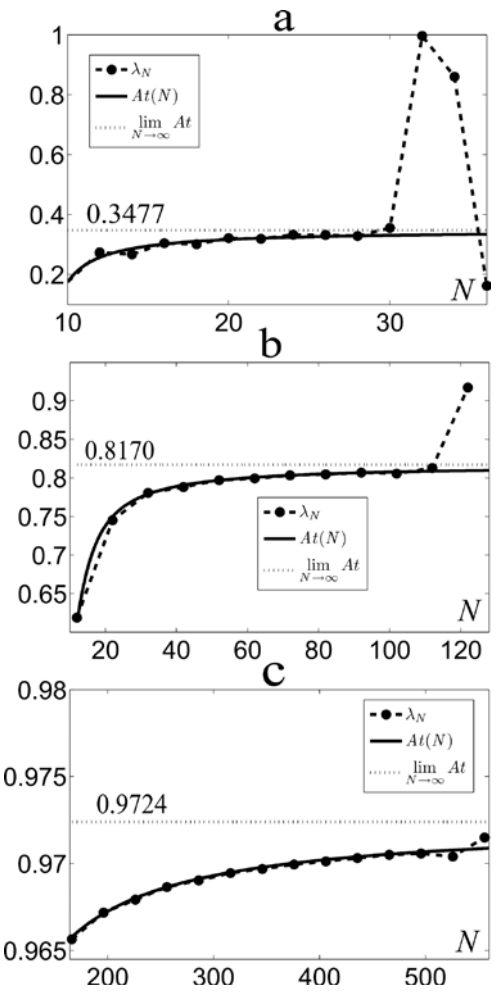

Fig. 6: Values of λ_N (large dots), graph of the function $At(N)$ (solid line), limit value $\hat{q}$ (dots) for the cases $r_0 = 0.2\ (a), r_0 = 0.01\ (b), r_0 = 0.0002\ (c)$

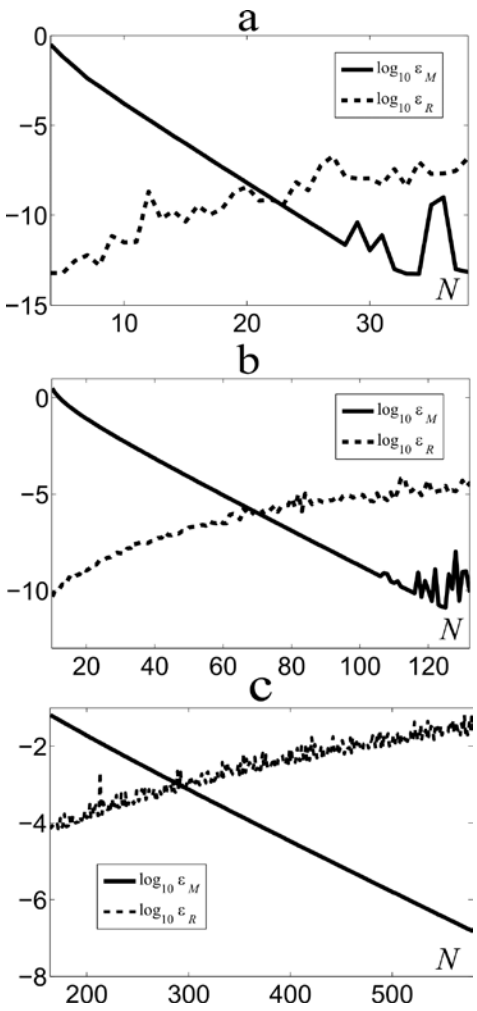

Fig. 7: Values of $\log_{10}\varepsilon_M$ and $\log_{10}\varepsilon_R$ for the cases $r_0 = 0.2\ (a), r_0 = 0.01\ (b), r_0 = 0.0002\ (c)$

References:

[1] Altuhov Yu. A., Gusev A. S., Pyshnograi G.V. *Introduction to the Mesoscopic Theory of Flowing Polymer Systems*. Barnaul: Altai State Pedagogical Academy, 2012 (in Russian).

[2] Pokrovskii V. N. The Mesoscopic Theory of Polymer Dynamics. *Berlin: Springer*, 2010. 256 p.

[3] Vinogradov G. V., Pokrovskii V. N., and Yanovsky Yu. G. Theory of Viscoelastic Behavior of Concentrated Polymer Solutions and Melts in One-Molecular Approximation and its Experimental Verification. *Rheol. Acta.*, Vol. 7, 1972, pp. 258–274.

[4] Pyshnograi G. V. , Gusev A. S., and Pokrovskii V.N. Constitutive equations for weakly entan-gled linear polymers. *Journal of Non-Newtonian Fluid Mechanics*. Vol. 164, No. 1–3, 2009, pp. 17–28.

[5] Blokhin A. M., Semisalov B. V. A stationary flow of an incompressible viscoelastic fluid in a channel with elliptic cross section, *Journal of Applied and Industrial Mathematics*, Vol. 9, No. 1, 2015, pp. 18–26.

[6] Blokhin A. M., Semisalov B. V., Shevchenko A. S. Stationary solutions of equations describing the nonisothermal flow of an incompressible viscoelastic polymeric fluid, *Math. Modeling*, Vol. 28, No. 10, 2016, pp. 3–22 (in Russian).

[7] Blokhin A. M., Kruglova E. A., Semisalov B. V. Steady-state flow of an incompressible viscoelastic polymer fluid between two coaxial cylinders. *Computational Mathematics and Mathematical Physics*, Vol. 57, No. 7, 2017, pp. 1181–1193.

[8] Semisalov B. V. A fast nonlocal algorithm for solving Neumann–Dirichlet boundary value problems with error control, *Vychisl. Metody Programm*, Vol. 17, No. 4, 2016, pp. 500–522 (in Russian).

[9] Achieser N. I. *Theory of Approximation*, New York: Frederick Ungar Publishing Co, 1956, 307 p.

[10] Canuto C., Hussaini M.Y., Quarteroni A., Zang Th. A. *Spectral Methods: Fundamentals in Single Domains*, Berlin Heidelberg: Springer, 2006, 565 p.

[11] Babenko K. I. *Fundamentals of numerical analysis*. Fizmatlit, Moscow, 1986, 744 p. (in Russian).

[12] Trefethen L. N. *Approximation Theory and Approximation Practice*, SIAM, 2013, 295 p.

[13] Boyd J. *Chebyshev and Fourier Spectral Methods.* Second Edition. University of Michigan, 2000, 594 p.

[14] Rump S.M. Verification Methods: Rigorous Results using Floating-point Arithmetic, *Acta Numerica*, Vol. 19, 2010, pp. 287–449.

[15] Alefeld G., Herzberger J. *Introdution to Interval Computations*, N.Y.: Academic Press, 1983, 352 p.

[16] Godunov S.K., Antonov A.G., Kiriljuk O.P., Kostin V.I. *Guaranteed Accuracy in Numerical Linear Algebra*, Springer Netherlands, 1993, 252 p.

[17] Demmel J.W. *Applied Numerical Linear Algebra*, SIAM, 1997, 431 p.

[18] Bernstein S. N. *Sur l'Ordre de la Meilleure Approximation des Fonctions Continues par*

des Polynomes de Degre Donne,Mem., Acad. Roy., Belg., 1912.

[19] Stoer J., Bulirsch R. Introduction to Numerical Analysis, *Springer-Verlag New York*, Inc., 2nd edition, 1993, 660 p.

[20] Gornov A. Yu., Tyatyushkin A. I., Finkelstein E. A. Numerical methods for solving applied optimal control problems, *Computational Mathematics and Mathematical Physics*, Vol. 53, Issue 12, 2013, pp. 1825–1838.